



SAFETY AND TRANSPORT
VEHICLES AND
AUTOMATION



WP2 SAMPO – Online condition monitoring techniques - Dielectric Properties

Henrik Toss

RISE Report : P114242.AP02DP01.A01

Content

Content	2
Background	3
Goal of the study	3
Methods	4
Waveguide method	4
Cable measurements.....	5
Parallel plate impedance measurements	7
Results and discussion	9
Waveguide method	9
Cable measurements.....	11
Parallel plate impedance measurements	22
Conclusions	24
Waveguide method	24
Cable measurements.....	24
Parallel plate impedance measurements	25

1 Background

Changes in the chemical structure and overall composition of the materials are likely to affect the dielectric properties and there are previous examples where changes in dielectric properties have been linked to aging of polymeric materials [1] [3]. The effects of ageing on the dielectric behaviour of the materials in question could be measured using e.g. impedance/dielectric spectroscopy. A very convenient method to monitor the status of rubber or polymer materials would be to measure material changes online, i.e. more or less continuous measurements or non-destructive sampling of the materials as they are fulfilling their intended function. If there are large enough changes in dielectric behavior of the materials that can be directly related to the ageing process, it should be possible to follow these changes e.g. using resonant structures such as antenna dielectric sensors [2]. By broad band frequency mapping of the dielectric behavior of the materials under test, more narrowband antenna like structures could hopefully be designed to fit the frequency providing the highest sensitivity and ease of use at lower cost. Placement, environmental factors and calibration of sensors would likely also be issues necessary to address as well as monitoring humidity and temperature to avoid overlapping effects of moisture content and degradation of the monitored polymers. This strategy towards assessment of polymer ageing has been part of Task T2.1 - Online condition monitoring techniques in the SAMPO project.

To our knowledge, there is not any one method for characterization of electromagnetic properties of materials that would work for all types and shapes of materials, in any environment, and for all frequencies. It should also not be expected that such a method could arise. The properties under investigation are highly frequency dependent, different material changes may only be visible in material specific frequency regions, and chemical changes may even affect the electromagnetic properties in different directions for different frequencies. It is thus impossible to make any generalized statement or predict of how materials change with ageing without having more information about their constitution. Choosing a suitable measurement method also depends on the shape of the sample, as well as the location and environment where it is expected to be found. The type of information mentioned here has not been made available during the project and it is thus very difficult to assess the usability of any specific method for any specific material. The strategy has instead been to investigate the materials available, with any methods available that would fit that sample geometry. During 2022 material samples in the form of insulated cables were introduced.

2 Goal of the study

The goal of this study was to assess if the accelerated ageing performed within the project induced measurable dielectric changes in some of the rubber materials and, if possible, identify specific frequency regions with more pronounced as well as systematic changes. We also wanted to investigate the feasibility of the concept of online monitoring of dielectric changes in similar rubber materials over extended periods of time.

3 Methods

3.1 Waveguide method

As an alternative to the previously investigated dielectric probe method, it was decided to try a method for determining the dielectric properties based on placing a sample inside a waveguide and calculating the electromagnetic properties according to the Nicholson-Ross-Weir Conversion Process [4] [5] [6]. The method was first evaluated on a lab bench and the results can be found as a separate report (“Electromagnetic material properties of rubber blends”, 2021).

This method has less resemblance, than the dielectric probe, with the initially proposed antenna sensor but assesses the same properties. The waveguide used will set the boundaries for the frequency space for which the method is valid and to investigate a wider range of frequencies, several different waveguides would thus need to be used. It has previously in the project been stated that higher frequencies are of more interest as they are expected to be less sensitive to the ambient humidity. We believe this was motivated by some samples being prone to absorb some of the ambient humidity and that the dielectric constant of water is quite high at low frequencies ($\epsilon_r \approx 80$) but rapidly decreases at higher frequencies [7] and is thus less likely to dominate the effective permittivity of e.g. polymeric materials with dielectric constants below 10. For high precision results the waveguide measurements are dependent on proper measurement of mechanical lengths related to the thickness and placement of the sample in the waveguide. This means that it will likely be more prone to errors at higher frequencies where a small error in mechanical length will be larger relative to the wavelength.

A benefit of using the waveguide measurement setup for sample material tests is that the equipment has a higher temperature tolerance, than the previously used dielectric probe, and the measurements can thus be performed at higher temperatures which should yield faster results.

The material investigated was a commercial grade Ethylene Propylene Diene M-class rubber (EPDM, cf. grade 3, task 1.3).

The setup was first tested for stability by setting everything up in the oven, where the actual experiment was to take place, and measuring on the sample at room temperature for ~7 days.

After this, the sample was removed and the oven, with waveguide, calibration kit, and sample holder inside, was heated to the ageing temperature. Two different temperatures were used for online monitoring of the ageing polymer, 80 °C and 90 °C. When the temperature had been stabilized the setup was recalibrated.

The room temperature sample was installed in the warm setup and measurements were started immediately. The initial heating of the sample should be taken into account when analyzing the data.

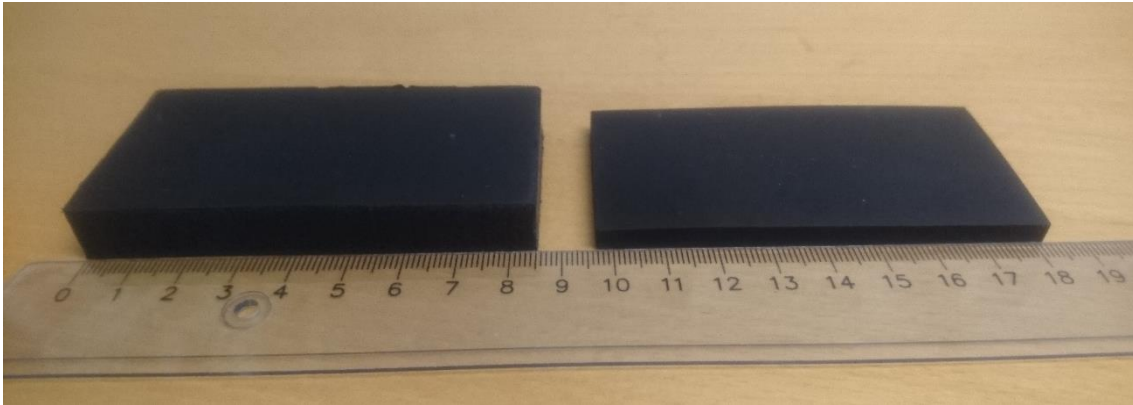


Figure 1. Rubber samples for waveguide measurements. The thicker sample, to the right, was aged at 80 °C. The thinner, to the left, was aged at 90 °C.

The project had access to two sample pieces of suitable size and shape. The first was measured at 90 °C as this was assumed to yield fairly quick results. It was indicated in discussions with Task T2.2 that it would be preferable to perform the measurements at slightly lower temperatures as there were indications of some difference in how the samples aged. Online measurements were thus also performed at 80 °C. Unfortunately, the measurement setup was disturbed during the lower temperature measurement, and we could only retrieve reliable data for the first ~5 days of that measurement cycle. The two samples were, in these measurements, also of a different thickness. The method used should compensate for the thickness, but it may still have an impact on the results. The increased thickness will mean that the surface regions of the sample will constitute a smaller part of the entire sample. It will also take longer for the entire sample to reach the set temperature and possibly reactive species, e.g. oxygen, would have a longer path to travel from the surface to the centre of the sample.

3.2 Cable measurements

The material that was to be investigated was a protective rubber insulation (chlorinated polyethylene) (CPE) around a coupled wire as that material has also been subject to mechanical testing. It is, in fact, the mechanical breakdown that is of main interest, and changes in the electromagnetic properties would only serve as possible indicators if relatable to the mechanical changes.

3.2.1 Cross talk measurements

Since little was known about the use of the cables, it was decided to try to use some generalized method of measurement related to the cable impedance. Initially, a method used for investigating shielded cables, by inspecting cross-talk, was tried.

In the original setup the investigated cables are, in a parallel pair, suspended at a constant distance over a ground plane, and each cable is in one end connected to a vector network analyzer (VNA), and in the other end terminated with a 50 Ω load. If the VNA is connected to the cables in the same end it is called Near End Cross Talk (NEXT), and in the opposite ends it is called Far End Cross Talk (FEXT). Our hope was that changes in the cable insulation could be traced to the cable matrix of the system.

The $50\ \Omega$ load terminations were chosen as it was assumed that would be closest to something that would be found in a real installation, and to have the same load at both ends of the cables (the port impedance of the VNA is $50\ \Omega$). To achieve a more distinct reflection it was also tested to instead measure with the end of the cables shorted.

Cables were cut to 0.5 m and the conductor wire pair, of each cable, were both soldered to N-contacts in both ends. These were in turn attached to two copper angle brackets attached to a large copper ground plane. The angle brackets were located opposite each other and adjusted so that the cables were in a stretched state between them, to ensure that the distance from the ground plane along the cables would be as constant as possible. The distance from the centre of the cable attachment points to the ground plane was 3.3 cm. There were very few samples available for measurement, likely because the cables were not initially intended for this type of measurement, but were rather left over from the mechanical testing. With this setup we ended up measuring only one aged cable and two unaged cables. The different combinations of these cables were all investigated. To somewhat minimize the influence of mounting the cables differently, or rather to introduce a new error for each individual measurement, we removed the cables and remounted them in a new position between different measurements as well as measurement types.

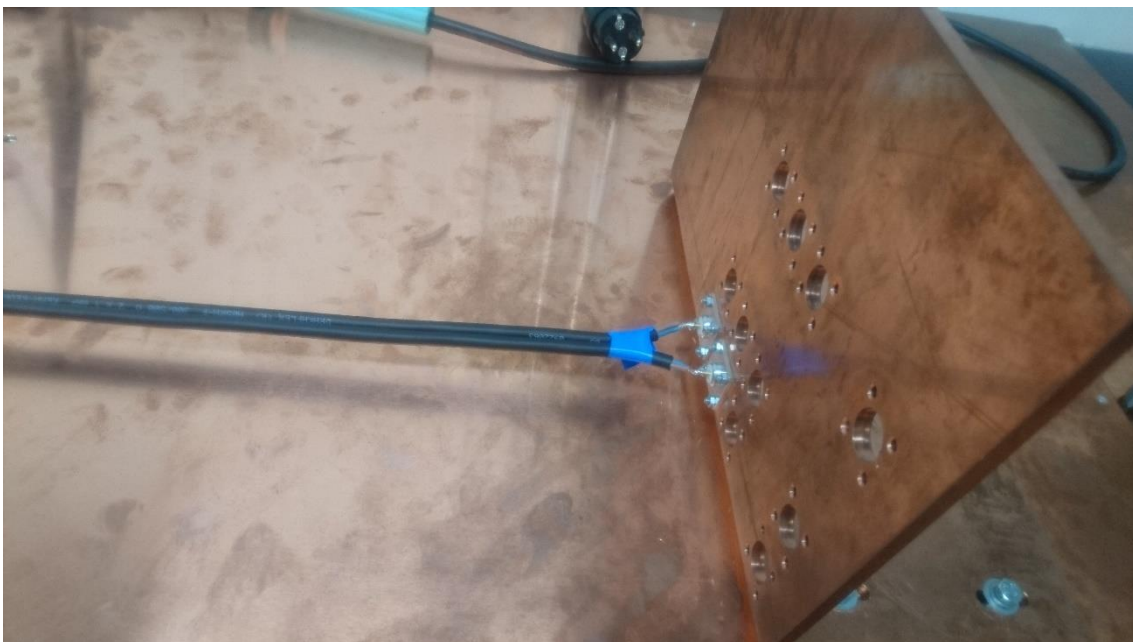


Figure 2. Cables mounted and taped to run parallel above the ground plane. The connectors are located on the outside of the copper angle brackets. Each of the wires is connected to the VNA in one end and a termination ($50\ \Omega$ or short) is connected to the other end of that wire. If the wires are connected to the VNA at the same end, we call the measurement NEXT. If they are connected at opposite ends, we call it FEXT.

3.2.2 Reflectometry

To isolate the effect on each cable sample, they were also measured with only one cable mounted at a time. In this case we shorted the cable in the far end to achieve a well-defined reflection.

3.3 Parallel plate impedance measurements

Some initial low frequency impedance measurements were performed on neoprene rubber samples cut from membranes (cf. task 1.1).

The rubber sample is sandwiched between two copper electrodes to create a structure similar to a parallel plate capacitor. The materials were characterized over the interval $0.1\ \text{Hz} - 20\ \text{MHz}$. Unaged samples were characterized as well as samples aged at 90 or $100\ ^\circ\text{C}$ for two weeks. The impedance is normalized by the overlapping area of the electrodes and the thickness of the samples.

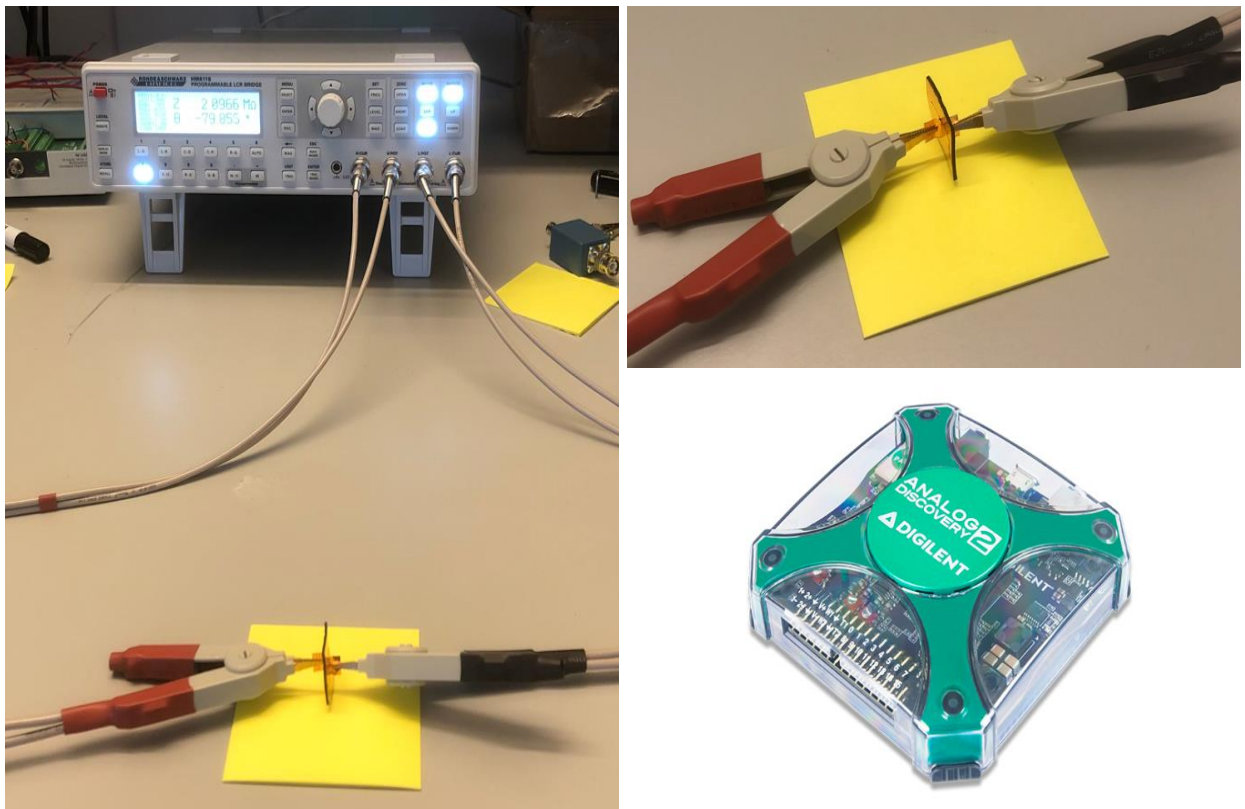


Figure 3. (Left) LCR Hameg HM8118 Rohde & Schwarz was used to measure impedance in the frequency range of $20\ \text{Hz}$ to $100\ \text{kHz}$, (Right top) sample configuration (plate capacitance) with electrodes between the sample, (Right bottom) Analog discovery 2 that was used for impedance measurements between $0.1\ \text{Hz}$ and $20\ \text{MHz}$.

4 Results and discussion

4.1 Waveguide method

The stability check of the measurement set-up showed that there was some drift in the results and revealed some form of periodic low frequency background signal which is estimated to possibly introduce an error of $< \sim 0.4\%$ on the calculated permittivity value of the specific material under test. Even though the noise could be considered low, a simple low pass (Moving Average) filter, corresponding to approximately 50 minutes, was applied to filter out background noise.

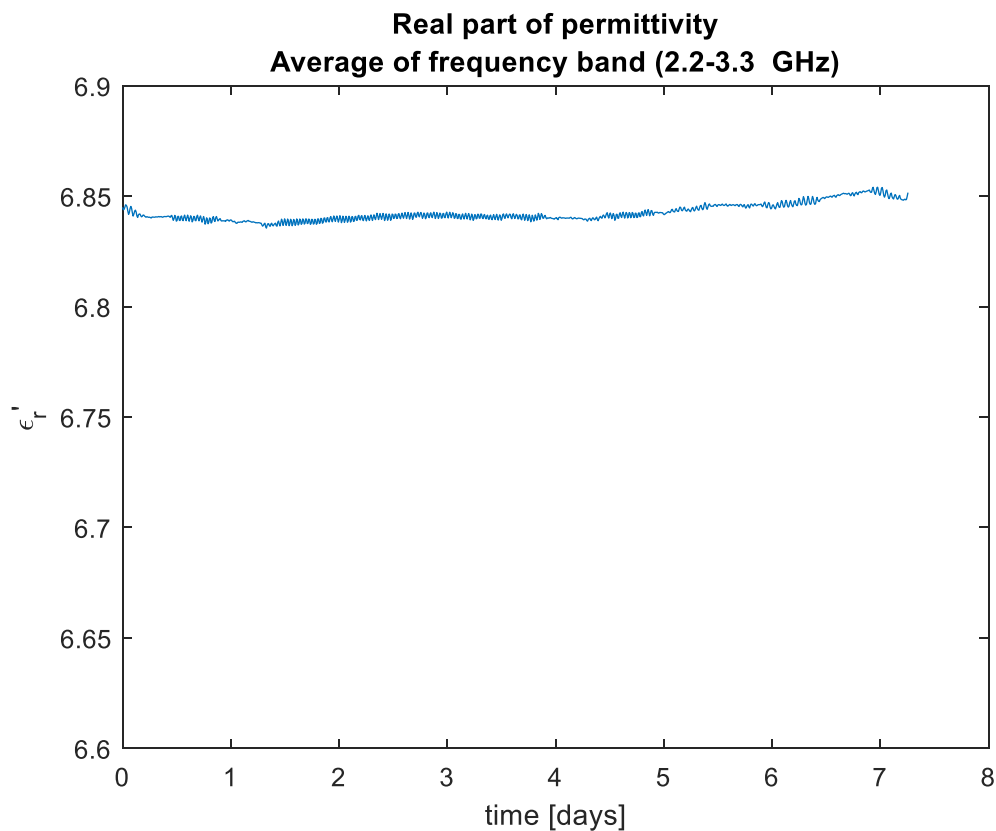


Figure 4. EPDM real part of relative permittivity at room temperature. Online measurement over one week.

The stability of the method and the material over one week at room temperature can be seen in Figure 4.

For the online measurements at the more elevated temperature (90 °C), changes to the material properties appear to start immediately (see Figure 5). The early changes in permittivity are also more dramatic and properties appear to level off after a little more than a week and an apparent change of $\sim 3\%$ in permittivity from $\epsilon_r \approx 6.8$ to $\epsilon_r \approx 6.6$.

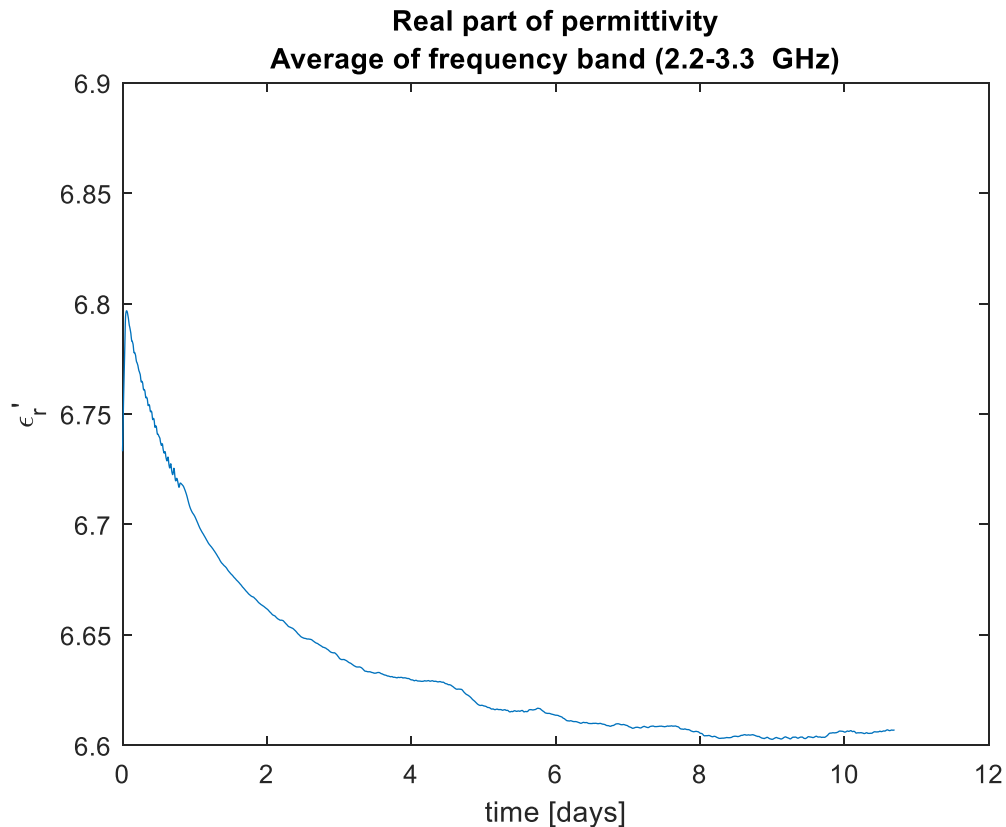


Figure 5. EPDM real part of relative permittivity at 90 °C. Online measurements

There were some differences observed for the measurements at 80°C (Figure 6) as compared to those at 90°C. First, the initial increase in permittivity that can be seen for both temperatures is noticeably slower for the lower temperatures. This could likely be explained by the sample, used for the 80°C measurement, being of about twice the thickness, thus taking longer for the entire sample to get warm. Second, the initial permittivity appears much lower, even from the very start. It is difficult to speculate as to why this is, but the fit of this sample to the sample holder was not as good and it is possible that there could have been a small misplacement in the sample holder or small air gaps along one or more of the sample edges leading to this error. We still believe the overall behaviour could be used as an indicator of how the samples would change with ageing. After the initial increase of permittivity, it starts to fall off also for this temperature, but at a much slower rate. It would have been interesting to see if this trend would continue and could be compared to the measurements at higher temperatures, but this was not possible due to lack of test materials as well as the equipment not being possible to book for these prolonged times.

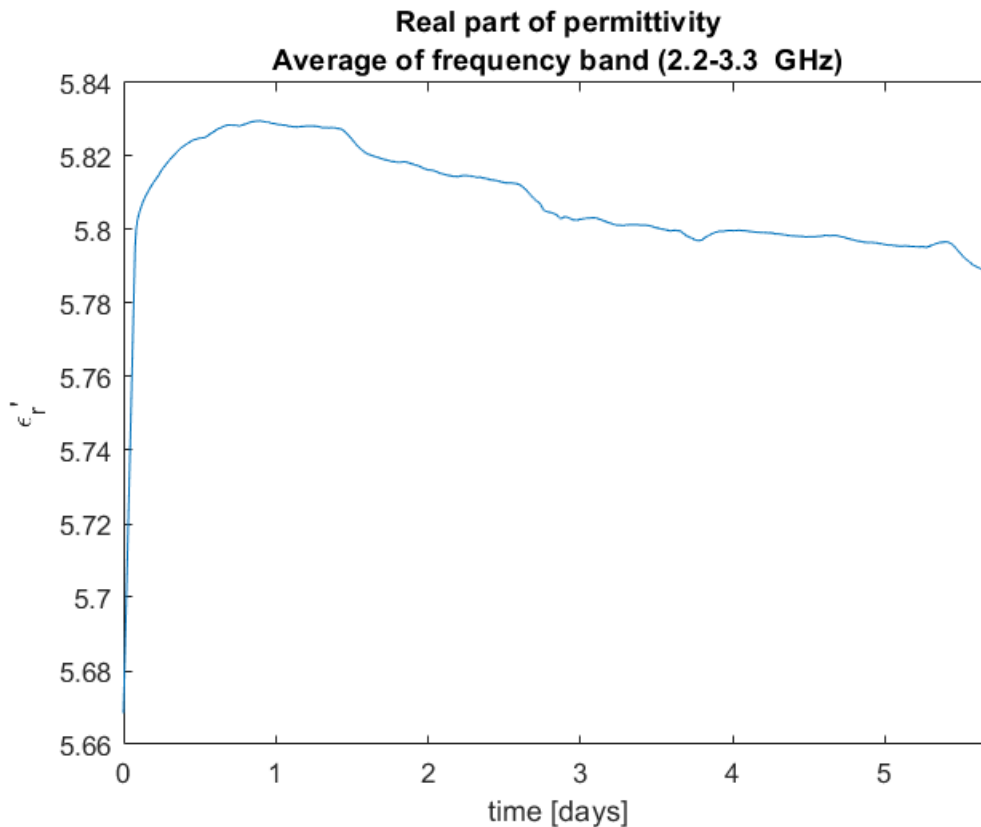


Figure 6. EPDM real part of relative permittivity at 80 °C. Online measurements

4.2 Cable measurements

Several measurements of the same type have been performed. In the figures of this section, it is the (linear) mean of the measurements of the same type that are presented as representations of that measurement type.

4.2.1 Cross talk measurements

Two-cable S-parameter measurement results can be seen in Figure 7-Figure 12. When the aged cable is included in the measurements, it is attached to port 2 of the VNA. When inspecting the frequency response from the measurements where the cables are terminated with a 50 Ω load (Figure 7-Figure 9), there is only a very small difference in location of frequency dips of S11 as well as S22, even though they are measuring the response on the two different cables in the measurement. Upon first inspection, the first clearly pronounced dip can be found around 270 MHz. This corresponds to a wavelength in air of about 1.1 m, which coincides quite well with twice the cable length (2*0.5 m). This would mean that the effective permittivity is only slightly higher than that of air. The difference in mean location (frequency) between the Aged-Unaged (A-U) cable pair as compared to the Unaged-Unaged (U-U) pair is around 1% for both S11 and S22 both when looking at NEXT as well as FEXT. This would correspond to a change in dielectric constant of about 2%. This change is too small to determine if it is significant without

performing more measurements. It is interesting to note that the reflection coefficient changes in a similar manner on both ports (S_{11} , S_{22}), even though it is only the cable on port 2 that is changed to an aged cable. Upon closer inspection, there does appear to be the tendency of a smaller dip in S_{11} and S_{22} a slightly lower frequency and yet again at what could be twice that lower frequency. At these, less pronounced dips, the frequency shift between the U-U and A-U measurements appears to be larger and in the opposite direction from what was observed for the 270 MHz dip.

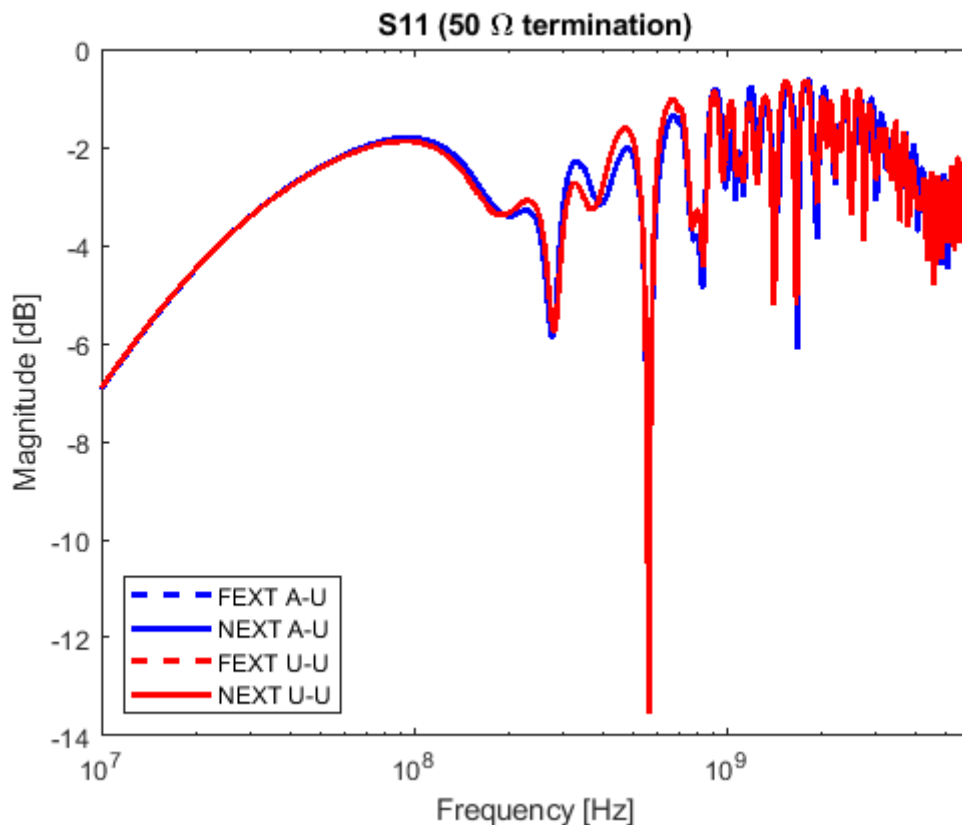


Figure 7. Far End Cross Talk (FEXT) and Near End Cross Talk (NEXT) S_{11} of a system of two parallel cables above ground plane where the end of each cable is terminated with a 50Ω load. Line colour indicate the type pairing of the two wires. Blue – one aged and one unaged cable. Red – two unaged cables. Aged cable is connected to port 2. The strong overlap between the data of the NEXT and FEXT measurements makes it difficult to discern the two different types of measurements.

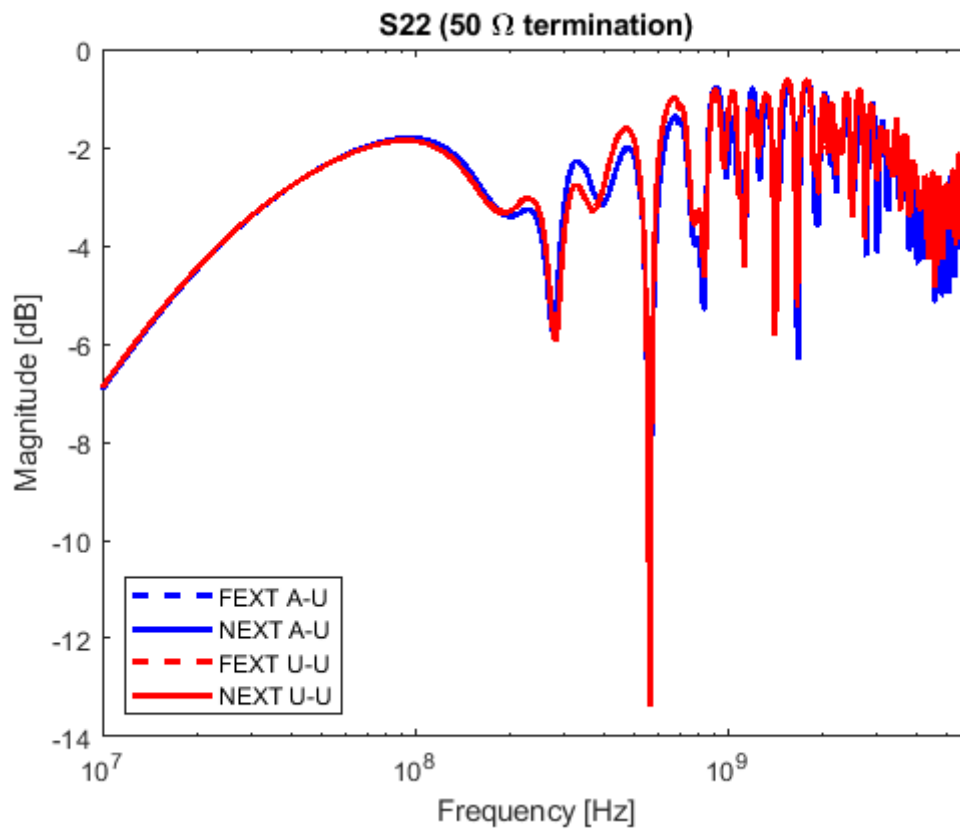


Figure 8. Far End Cross Talk (FEXT) and Near End Cross Talk (NEXT) S22 of a system of two parallel cables above ground plane where the end of each cable is terminated with a 50 Ω load. Line colour indicate the type pairing of the two wires. Blue - one aged and one unaged cable. Red - two unaged cables. Aged cable is connected to port 2. The strong overlap between the data of the NEXT and FEXT measurements makes it difficult to discern the two different types of measurements.

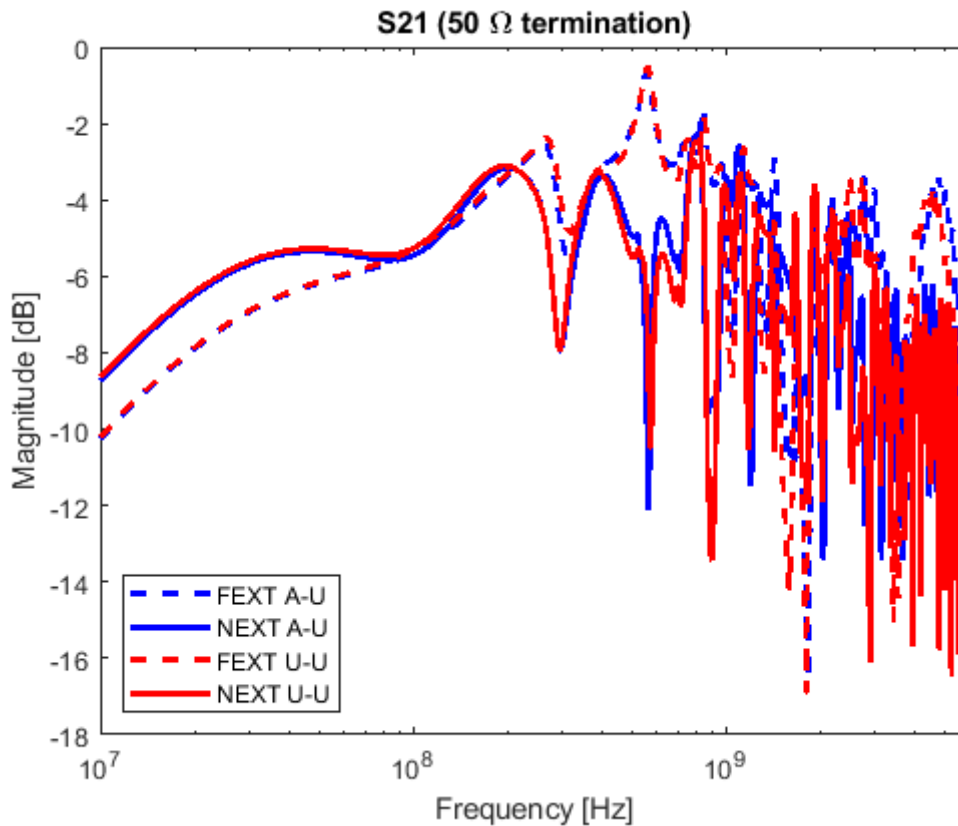


Figure 9. Far End Cross Talk (FEXT) and Near End Cross Talk (NEXT) S21 of a system of two parallel cables above ground plane where the end of each cable is terminated with a 50 Ω load. Line colour indicate the type pairing of the two wires. Blue – one aged and one unaged cable. Red – two unaged cables.

When the cable ends are shorted (Figure 10-Figure 12), the dips at lower frequencies emerges more clearly and the frequency is identified as of around 185 MHz. If this dip is due to a cable resonance it would correspond to an electrical length of about 0.8 m, which is much longer than the cable length of 0.5 m. If assuming this is indeed a resonance from the length of the cable, the effective relative permittivity can be calculated from this relation¹ and would then appear to be around $\epsilon_r \approx 2.5$ at this frequency.

The shift in frequency for the 185 MHz dip, when exchanging one unaged cable to an aged one, is more than 3%, which would correspond to a ~6.5 % change in ϵ_r . It would be expected to find another dip at the next resonance, which should be possible to find at about twice the frequency of the first frequency dip. There is indeed a dip close to 380 MHz. The shift in frequency at this dip is even more pronounced and would correspond to a change in epsilon of almost 10 %. Looking for the further resonances proved more difficult as the data becomes a little more noisy, but it was possible to identify dips at ~560 MHz with a similar shift between the aged and the unaged cables.

It should again be noted that the shift of the 185 MHz dip and the 270 MHz dip are in opposite directions. We are yet to find any good explanation for this.

¹ Assuming a relative permeability $\mu_r = 1$, electrical length L_e is simply $L_e = L * \sqrt{\epsilon_r}$

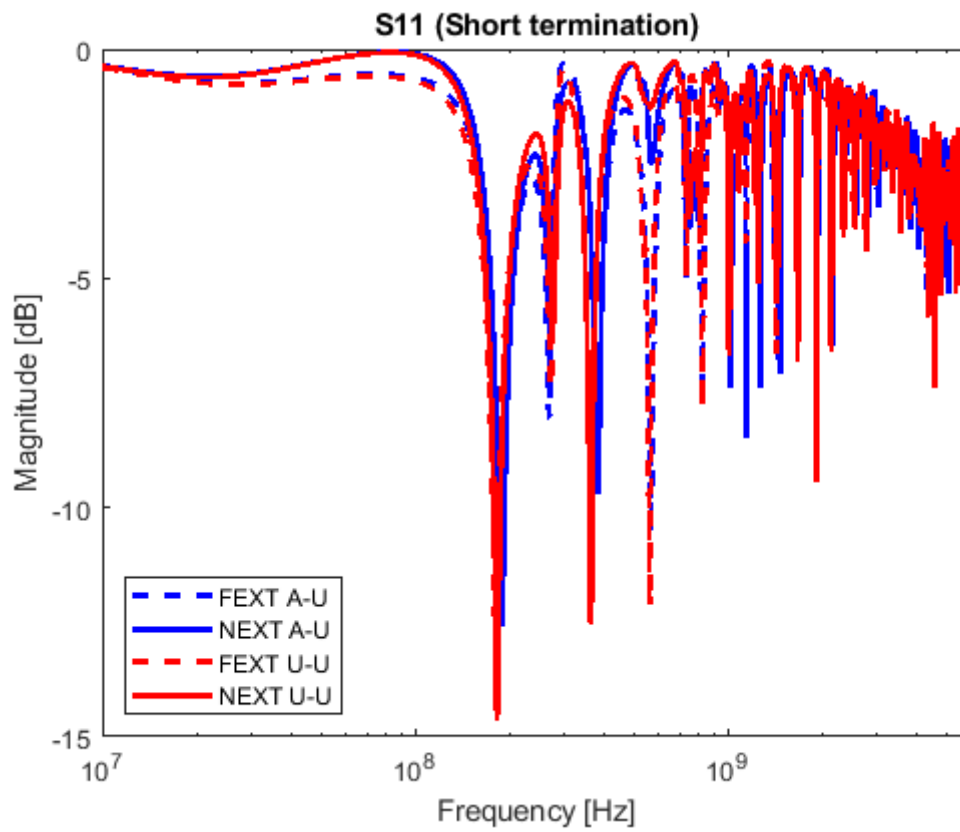


Figure 10. Far End Cross Talk (FEXT) and Near End Cross Talk (NEXT) S11 of a system of two parallel cables above ground plane where the end of each cable is terminated with a connection to ground (short). Line colour indicate the type pairing of the two wires. Blue – one aged and one unaged cable. Red – two unaged cables. Aged cable is connected to port 2.

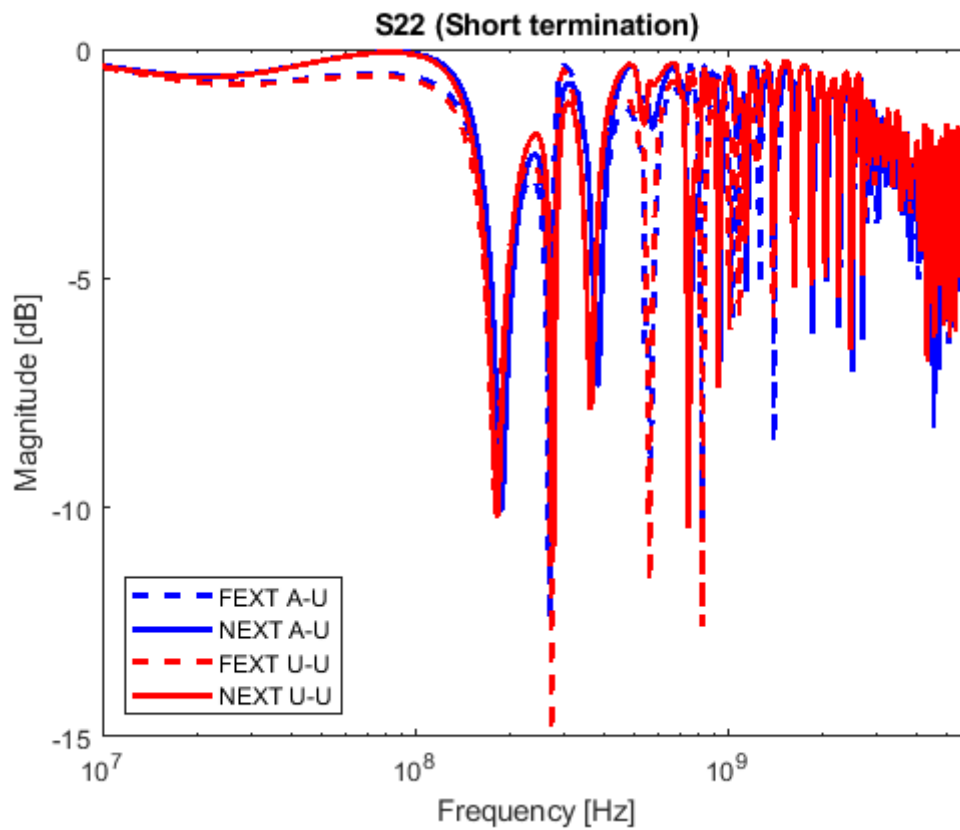


Figure 11. Far End Cross Talk (FEXT) and Near End Cross Talk (NEXT) S22 of a system of two parallel cables above ground plane where the end of each cable is terminated with a connection to ground (short). Line colour indicate the type pairing of the two wires. Blue – one aged and one unaged cable. Red – two unaged cables. Aged cable is connected to port 2.

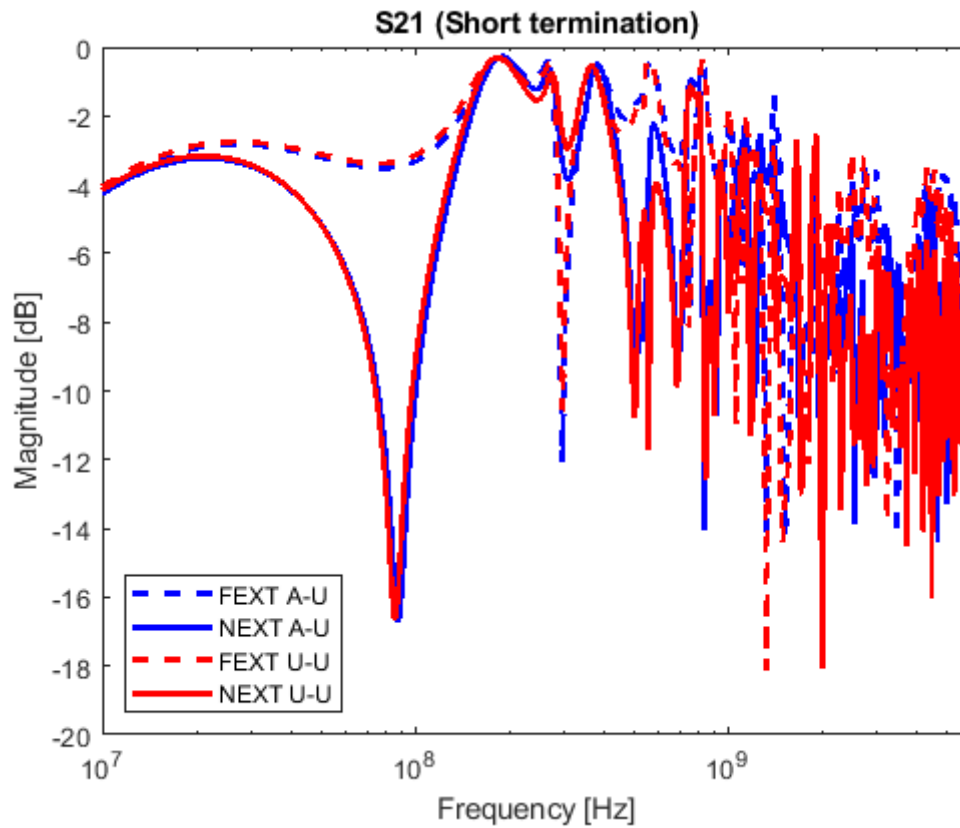


Figure 12. Far End Cross Talk (FEXT) and Near End Cross Talk (NEXT) S21 of a system of two parallel cables above ground plane where the end of each cable is terminated with a connection to ground (short). Line colour indicate the type pairing of the two wires. Blue – one aged and one unaged cable. Red – two unaged cables.

4.2.2 Reflectometry

When looking at the S11-data (Figure 13) from the cables mounted one at a time, the difference between the aged and the unaged cables appears almost non-existent. The lowest frequency with an identifiable dip at is here clearly found around 270 MHz. The frequency shift of the dips in S11 is at most found to be less than 0.5 % which is probably too small to consider significant even though the direction of the shift is consistent with what was observed for the cross talk measurements at the 270 MHz dip.

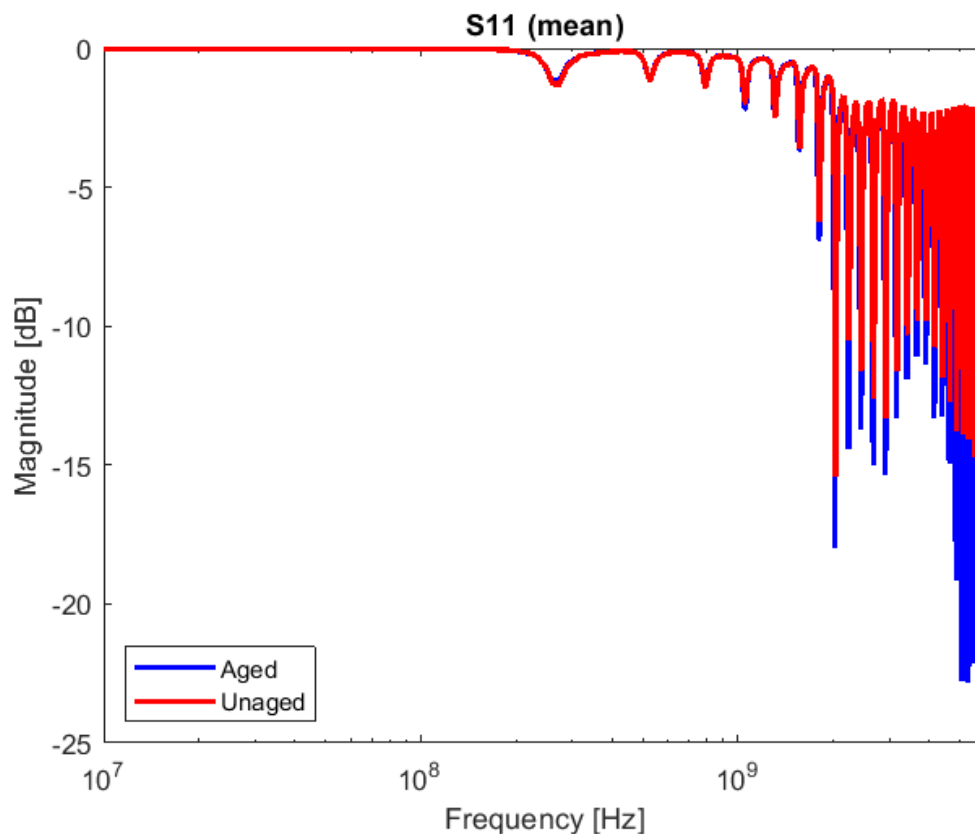


Figure 13. S11 of single cables above ground plane where the end of the cable is terminated with a connection to ground (short). Line colour indicate the type of wire. Blue – aged cable. Red – unaged cable.

It is possible to try to compare the electrical length of the cables by transforming the data from frequency domain to time domain (Figure 14-Figure 17). The frequency sampling was in some cases logarithmically spaced and a non-uniform inverse DFT had to be used, which could introduce some artifacts (e.g. ringing). The time data was scaled by the speed of light to instead show electrical distance travelled along the cable. As S11 (and S22) is the reflected signal at each port, the distance is here also divided by two to compensate for the signal travelling to and from the reflection point. There is an initial large reflection due to impedance mismatch at the very contact point closest to the VNA. The main reflection then shows up at a distance of a little more than 0.5 m, as the electrical length of the cable is slightly more than the mechanical length (signal velocity is slower than the speed of light). Similar reflection patterns can be seen reoccurring with decreasing signal strength at n-times the distance to the main reflection as the signal travels back and forth along the cable. The reflection appears somewhat indistinct, which could be due to the state of the cable close to the contacts where it has been stripped and soldered. This may add to the explanation why the data becomes a little more chaotic at higher frequencies

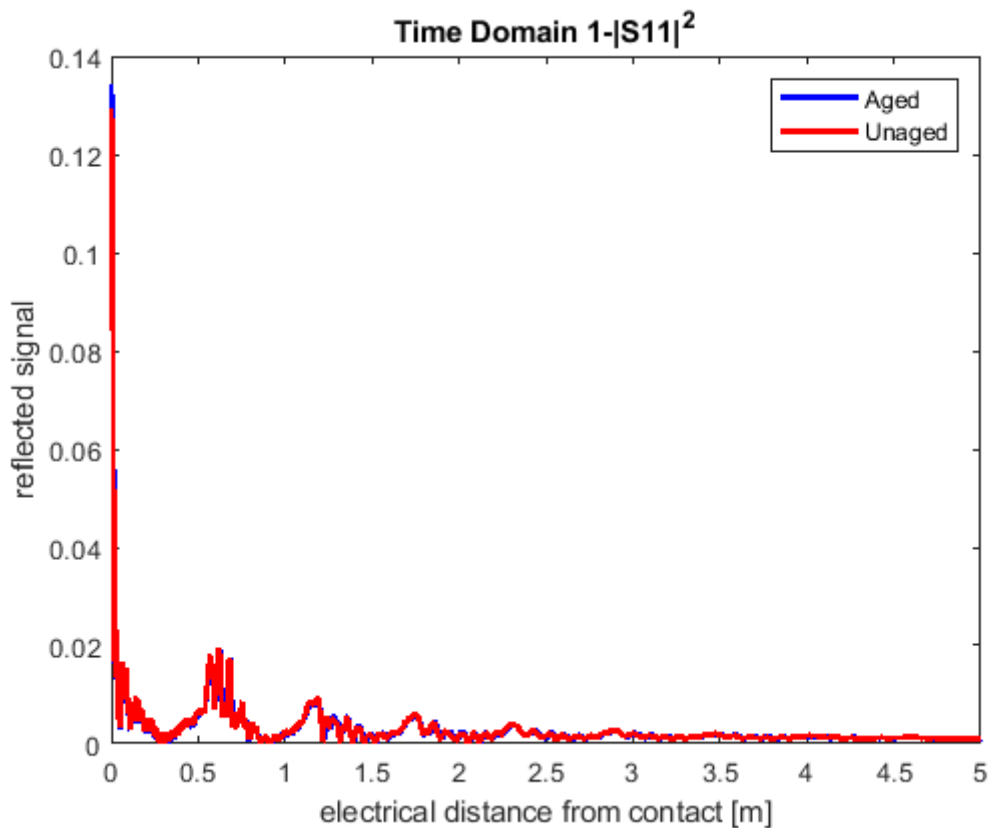


Figure 14. Reflected signal from along the wire calculated from S11 frequency data. The underlying frequency data is logarithmically spaced which could explain some of the spread of the peaks and/or apparent ringing behaviour of the signal. For both aged (blue) and unaged (red) cables the reflection at the far end of the cable appears to occur at an electrical distance of ~ 0.6 m.

The single cable time domain measurements were repeated with lineary spaced frequency samples showing that the reflection in reality probably is a little bit sharper. The amplitude appears slightly lower for the aged cables, but that could probably be attributed to a differences in the contacts. As S11 is a relation between the incident and reflected power waves it can never add up to more than 1 and the amplitudes of peaks further down the cable will thus be affected by a stronger initial reflection.

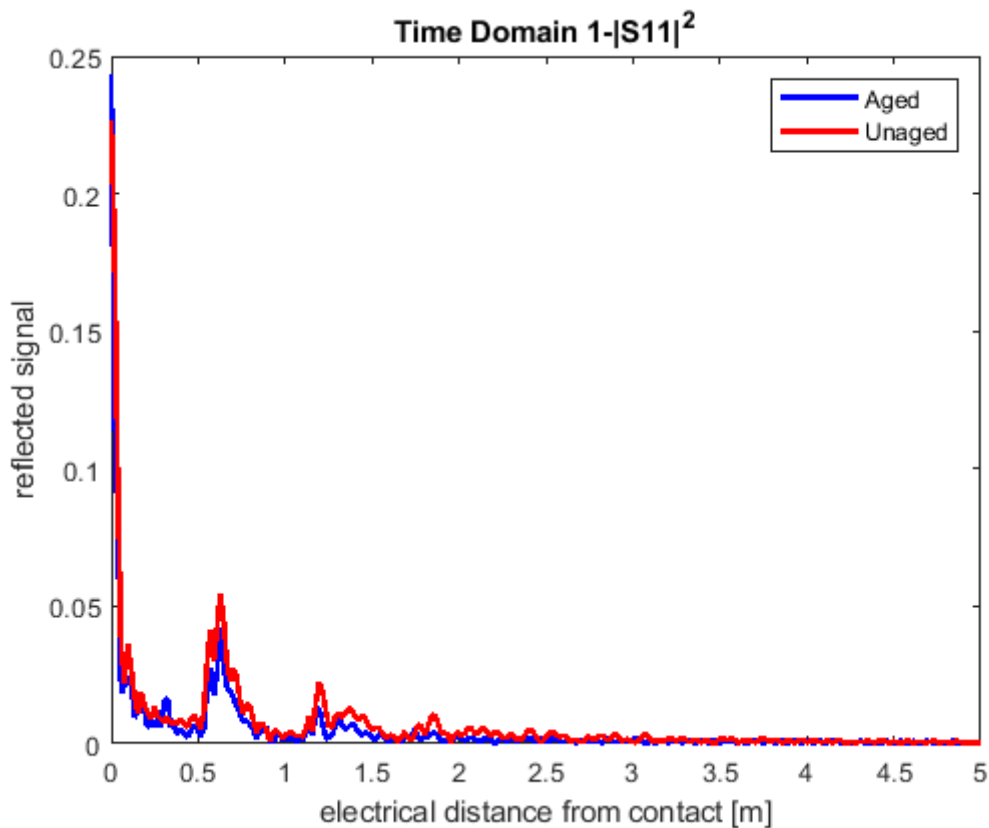


Figure 15. Reflected energy along single cables calculated from linearly spaced frequency data. The initial contact show a quite large reflection, but the first reflection further in on the cables is at ~ 0.6 m. The difference in amplitude between the curves is likely due to the first reflection being larger for the aged sample. This is likely an effect of the contact rather than the sample.

It is also possible to transform the reflected signal of the cross-talk measurements to try to locate the reflections (Figure 16-Figure 17). The frequency samples in these measurements were all log-spaced which could introduce artefacts and one should be careful drawing conclusions. This was unfortunately realized too late and more time would be needed to repeat the experiment with more carefully chosen measurement parameters.

For the dual cable measurements there appears to be more reflections possible along the entire length of the cable. By this, we are referring to the more spread out initial values from $\sim 0-0.4$ m. This effect is more pronounced for the FEXT-measurements. The largest reflection (after the first contact reflection) is indeed located at ~ 0.8 m, but there appears to be another small peak, approximately at the same location as where it was found for the single cable measurements ($\sim 0.5-0.6$ m)

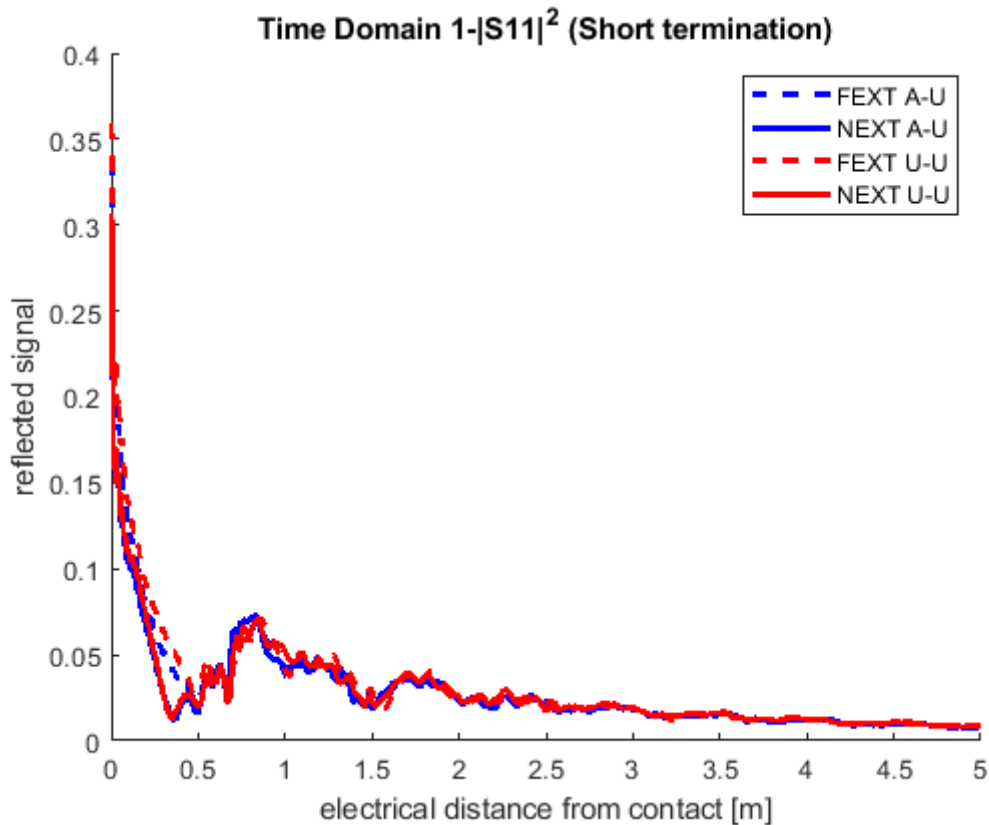


Figure 16. Reflected energy along the cable length with a second cable attached in contact. The measurements are named by the measurement type (FEXT/NEXT) and cables involved (Aged-Unaged/Unaged-Unaged). The entire length of the cable appear to show some reflected energy, but peaks can be seen at ~ 0.6 m and ~ 0.8 m

With the 50Ω load (Figure 17) it is much more difficult so see something in the data in this form. This should not be surprising as it would be expected to have fewer sharp transitions in impedance. There are however two noticable peaks. The first, again at ~ 0.5 - 0.6 m, and then another one at a little more than ~ 0.7 m. Again there is no large difference between the aged and unaged cables for the first peak while the second one moves in the same manner as was observed for the second peak in the measurements with the shorted ends (Figure 16). The shift is however slightly smaller than what was estimated looking at the frequency data. It is a lot more difficult to identify peak values of these reflections in the time domain as compared to some of the dips in the frequency domain.

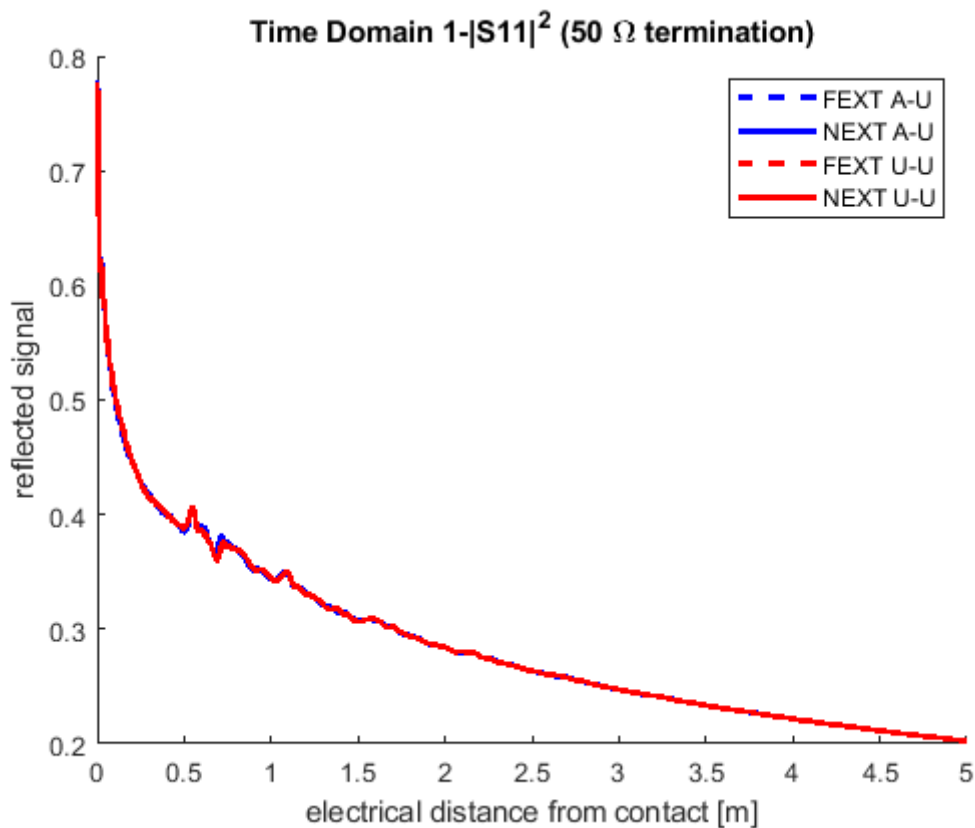
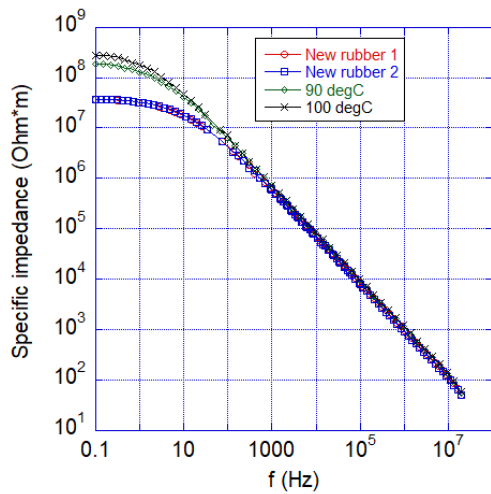


Figure 17. Reflected energy along the cable length with a second cable attached in contact. The measurements are named by the measurement type (FEXT/NEXT) and cables involved (Aged-Unaged/Unaged-Unaged). The entire length of the cable show reflected energy, but small peaks can be noticed at ~0.6 m and ~0.8 m

4.3 Parallel plate impedance measurements

The results of sample ageing regarding the electrical impedance measurements are most clear at very low frequencies where the impedance appear to increase with increased ageing of the samples (2 weeks at 90°C and 100°C as indicated in Figure 18 compared to new rubber material). The phase angle also goes down at low frequencies indicating that the aged samples here show a more capacitive behaviour, while the pristine samples show a slightly more resistive behaviour. It cannot, at this time, be stated that this should be a general expectation without knowing the responsible ageing mechanism. These preliminary results non the less clearly show an effect of the aging on the impedance and thus renders the technique an attractive candidate for further investigation.

Normalized data with electrode area and sample thickness



Normalized data with electrode area and sample thickness

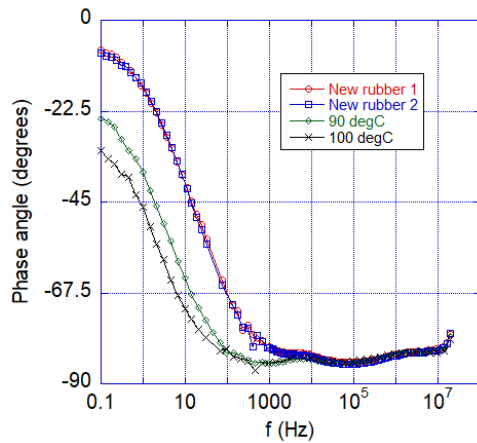
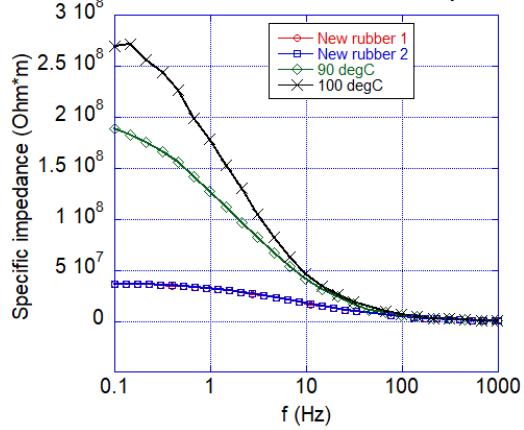


Figure 18. (top) Specific impedance (normalized with electrode area and sample thickness), (middle) zoomed in specific impedance at frequencies below 1 kHz and (bottom) phase angle (between excitation voltage and current), and versus excitation frequency. New rubber 1 and 2 are two fresh rubber samples and 90 degC and 100 degC are aged rubber samples aged in an oven for 2 weeks at 90 °C and 100 °C.

5 Conclusions

5.1 Waveguide method

Measurement results achieved can be seen as indications that the permittivity might yet prove a useful indicator for aging monitoring of some polymeric materials. The reason for the seen reduction in permittivity is yet to be investigated. It should thus not be expected that all materials would behave the same. If the change in permittivity is due to the consumption of some component, the trend might also change at later stages of ageing of the material. If the changes can be tied to some specific reaction, the method could thus prove to be very useful for understanding approximately where in the ageing process a well-known material could be. A weakness of the method would be that the entire course of ageing would likely need to be recorded for the method to be of much use. The changes here recorded are also fairly small. It remains to see if the changes are still large enough to use a passive structure, like a simple resonance circuit or antenna-like element, as a probe.

5.2 Cable measurements

Inspecting a single cable, as it was done here with the initial reflectometry methods, appears to have provided very little information. We have come to realize that this might be due to poor experimental design. As the distance from the cable to ground is much larger than the thickness of the cable the effective permittivity will likely be dominated by the air between the cable and the ground plane. It would probably be a good idea for future measurements to place the cables directly on the ground plane or to create a coaxial structure with ground surrounding the insulating material.

When two parallel cables were connected, we could however see some effect. This is probably because they are in much closer proximity and the effective permittivity between the cables is thus dominated by the CPE insulator instead of air. Even if only one cable was exchanged, from an unaged cable to an aged one, the effect could be observed in the reflection of both cables. We would suggest that this, together with the fact that it is more pronounced for the setup with shorted ends, shows that at least a part of the return current happens in the coupled conductor. If cables are mounted in a bundle, it could thus likely be useful to investigate them at least pairwise so that the effective permittivity of the cable will be dominated by the insulation material between the cables, and any distance to some other ground plane will be of less significance. In our measurements only one of the cables have been aged. If our argumentation is correct, the effective permittivity of the coupled cables should be dependent on the insulation material around both cables. If the other cable is aged as well, a larger effect on the effective permittivity should thus be expected.

The analysis could likely be improved by more in-depth circuit models to further understand the relation between the material changes and the effect on the measurements. This would likely also help in improving the measurement set-up. Unfortunately, there has not been time for this type of analysis as the samples arrived

quite late in the project. The number of available samples have unfortunately not been large enough to properly evaluate the method with valid uncertainty estimates. This would have to be changed if the work is to be continued.

The method could likely be adapted to an online measurement set-up with the cables under test located in a hot/warm environment.

5.3 Parallel plate impedance measurements

Even though there have previously been expressed concern towards working at low frequencies due to the, sometimes, humid environment and the effect the wet atmosphere might have on the measurements, the results from these measurements show a clearly visible effect of the ageing. This renders them interesting for further investigation. One way forward would be to try to construct equivalent circuits with elements related to the different ageing mechanisms.

References

- [1] Daily, C., 2015. Dielectric properties and degradation monitoring in polymer-matrix structural composites. Grad. Theses Diss. <https://doi.org/10.31274/etd-180810-3883>

- [2] Huang, H., 2015. Antenna Sensors in Passive Wireless Sensing Systems, in: Chen, Z.N. (Ed.), Handbook of Antenna Technologies. Springer Singapore, Singapore, pp. 1–34. https://doi.org/10.1007/978-981-4560-75-7_86-1

- [3] Li, L., 2011. Dielectric properties of aged polymers and nanocomposites (Doctor of Philosophy). Iowa State University, Digital Repository, Ames. <https://doi.org/10.31274/etd-180810-1135>

- [4] Rohde & Schwarz “Measurement of Dielectric Material Properties,” Application Note RAC0607-0019_1_4E, 2012.

- [5] A. M. Nicolson and G. F. Ross, “Measurement of the intrinsic properties of materials by time-domain techniques,” IEEE Trans. Instrumentation and Measurement, 19, 377-382, 1970.

- [6] W. B. Weir, “Automatic measurement of complex dielectric constant and permeability at microwave frequencies,” Proc. IEEE, 62, 33-36, 1974

- [7] Barthel, J. M. G. and Buchner, Richard. "High frequency permittivity and its use in the investigation of solution properties" Pure and Applied Chemistry, vol. 63, no. 10, 1991, pp. 1473-1482.



RISE Research Institutes of Sweden AB
Box 857, SE-501 15 BORÅS, Sweden
Telephone: +46 10 516 50 00
E-mail: info@ri.se, Internet: www.ri.se

Vehicles and Automation
RISE Report :
P114242.AP02DP01.A01
ISBN: